

# Reduced-order modeling for spacecraft thermal-structural applications

Derek Hengeveld<sup>1</sup>, Jacob Moulton<sup>2</sup>, David Tobin<sup>3</sup>, Ryan Vasas<sup>4</sup>, and Emmett Nelson<sup>5</sup>  
Redwire

*and*

Alice Liu<sup>6</sup> and Hume Peabody<sup>7</sup>  
NASA Goddard Space Flight Center

**Leveraging the speed of reduced-order models (ROMs), thermal analysis teams have previously had access to rapid optimization, sensitivity studies, rapid model correlation, and uncertainty quantification, to name a few. An advantage of the developed approach is its relative robustness, which enabled expansion to include structural models in addition to thermal models leading to both rapid thermal-structural and rapid structural-only analyses. This method was tested for a sample thermal-structural application and showed good performance. It was then applied to a complex NASA mission and showed how ROMs could be used to quickly evaluate system uncertainties. Finally, these methods were applied to a structural-only application and used to better optimize and understand the structural design.**

## Nomenclature

CSV	=	Comma Separated Values
FEMAP	=	Finite Element Modeling And Postprocessing
NASA	=	National Aeronautics and Space Administration
NASTRAN	=	NASA STRucture ANalysis
ROM	=	Reduced-Order Model
RST	=	Roman Space Telescope
R <sub>x,y,z</sub>	=	Rotations about the x,y,z directions
STOP	=	Structural-Thermal-Optical
UQ	=	Uncertainty Quantification
U <sub>x,y,z</sub>	=	Deformation in the x,y,z directions
VM	=	Von Mises

## I. Introduction

**R**EDUCED-order modeling has been successfully implemented for a broad range of spacecraft thermal analysis applications [1-5]. The developed approach creates surrogate models by accurately mapping (i.e., data fitting) select input factors to output responses. Leveraging the speed of reduced-order models (ROMs), thermal analysis teams have access to rapid optimization, sensitivity studies, rapid model correlation, and uncertainty quantification, to name a few. These methods have been successfully applied to such applications as the Mars 2020 Helicopter [6], Dream Chaser, and Vigoride programs to name a few. In addition to the speed of the ROMs, an advantage of the developed approach is its relative robustness. Since the method is based on sampling and data-fitting, it is not directly

---

<sup>1</sup> Senior Engineer, 2309 Renard Place SE, Suite 101, Albuquerque, NM 87106.

<sup>2</sup> Staff Engineer, 2309 Renard Place SE, Suite 101, Albuquerque, NM 87106.

<sup>3</sup> Mechanical Engineer, 8100 Shaffer Parkway, Suite 130, Littleton, CO 80127.

<sup>4</sup> Staff Engineer, 8100 Shaffer Pkwy, Suite 130, Littleton, CO 80127

<sup>5</sup> Director of Engineering, 2309 Renard Place SE, Suite 101, Albuquerque, NM 87106.

<sup>6</sup> Integrated Modeling Lead, Mail Stop 592, Goddard Space Flight Center, Greenbelt MD 20771.

<sup>7</sup> Staff Engineer, Mail Stop 545, Goddard Space Flight Center, Greenbelt MD 20771.

tied to a specific analysis tool or specific analysis type and can therefore be readily applied to others. With that in mind, the thermal ROM approach was expanded to a NASTRAN structural analysis workspace. The developed method was robustly built for various NASTRAN platforms (e.g., MSC Nastran, Autodesk® Nastran, and Simcenter Nastran). This method was then combined with thermal software (i.e., Thermal Desktop®). Thermal Desktop and NASTRAN models were paired to create multi-disciplinary ROMs. In this paper, a framework for developing and using Thermal-Structural ROMs is provided and several example cases illustrate their utility for both thermal-structural and structural-only applications.

## II. Reduced-Order Modeling

A thermal ROM approach to predict spacecraft output responses for a set of input factors was previously developed [2-5, 7, 8], and this approach was expanded into a software application called Veritrek®. It is based on intelligent sampling and robust data-fitting and provides a computationally efficient surrogate that accurately captures the effects of underlying high-fidelity thermal models (i.e., Thermal Desktop®). Recently, this method was expanded to not only include thermal effects but also structural impacts (e.g., thermally induced deformations). To demonstrate the Thermal-Structural ROM workflow, a sample problem was created (Figure 1) based on a simple optical component bracket (created in SolidWorks). The geometry and thermophysical properties were used to create both Thermal Desktop and NASTRAN models. A workflow was then used to capture both thermal and structural effects and create a resulting Thermal-Structural ROM (Figure 2). The Thermal-Structural ROM includes both thermal and structural inputs and maps these to x, y, and z deformations.

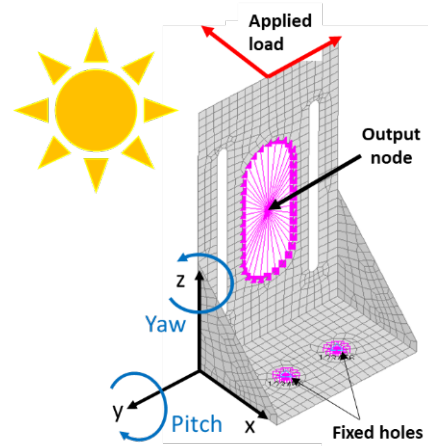


**Figure 1. Bracket NASTRAN model.**  
Model with applied load and output node locations.

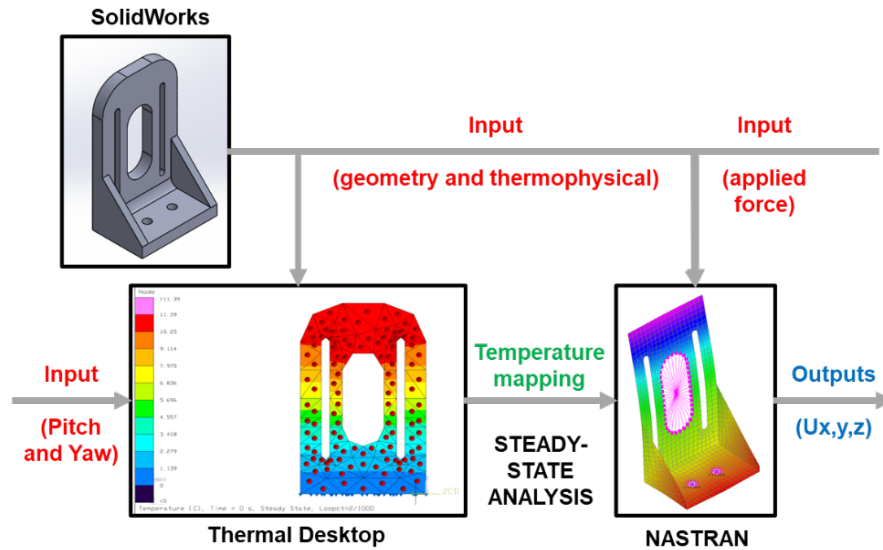


**Figure 2. Thermal-structural workflow.** A Thermal-Structural ROM was developed using both Thermal Desktop and NASTRAN models.

In Thermal Desktop, the bracket was placed at a single orbital position (i.e., -x Sun-pointing; +x Nadir-pointing) and the Pitch (i.e., rotation about y-axis) and Yaw (i.e., rotation about z-axis) were allowed to vary. By adjusting Pitch and Yaw, environmental loads vary primarily due to the change in incident angle of direct solar loading. Steady-state temperatures as a function of Pitch and Yaw were then mapped to the NASTRAN model using available Thermal Desktop mapping methods (i.e., Post Processing Data Mapper). An applied force from 0 to 100 lbf in both the -x and -y directions was then applied to the NASTRAN model. With updated temperature maps and applied force, the NASTRAN model was solved for x, y, and z deformations (i.e.,  $U_x$ ,  $U_y$ , and  $U_z$ ). Overall input factors and output responses for the bracket Thermal-Structural ROM were defined as follows:

- INPUT FACTORS (3 total):
  - Thermal model: Bracket pointing Pitch (0 to 90°) and Yaw (0 to 45°)
  - Structural model: Applied force in -x and -y directions (0 to 100 lbf)
- OUTPUT RESPONSES (3 total):
  - $U_x$ ,  $U_y$ , and  $U_z$  deformation (in inches) at a single node representing the optics mounting location

32 training data points, over the range of each input factor, were generated to develop the bracket Thermal-Structural ROM. An additional 12 test data points were used to test its accuracy. Figure 3 shows the performance of the Thermal-Structural ROM against training (Figure 3a) and test (Figure 3b) data. The ROM performed as expected. This is demonstrated by an exact fit of the training data (i.e., no noise noticeable in Figure 3a). Additionally, the test data shows good agreement between the test/truth and ROM results, although there is some noise (i.e., scatter) in the results (Figure 3b).

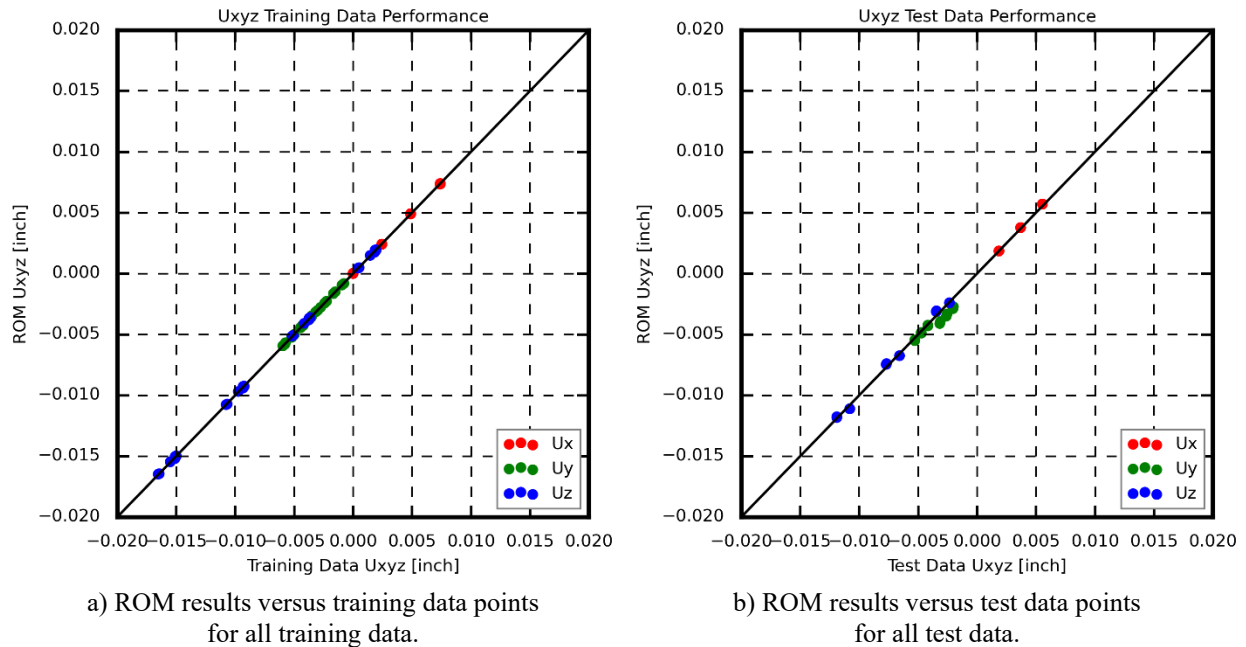
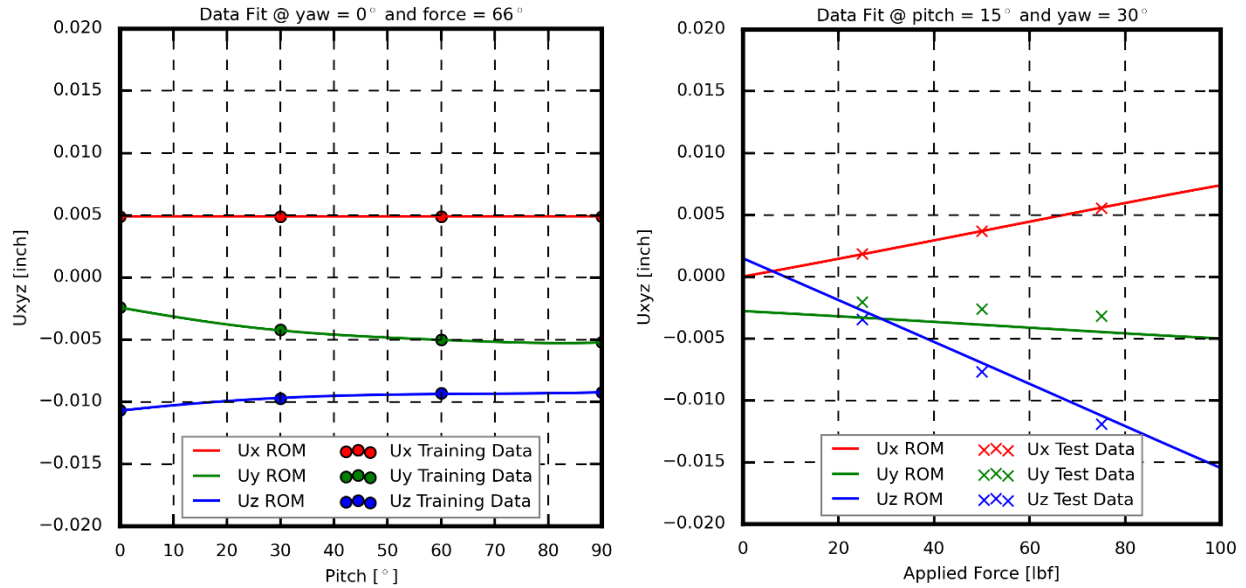


**Figure 3. Bracket Thermal-Structural ROM performance.** Performance of the simplified thermal-structural bracket ROM for both training and test data.

Performance sweeps were conducted to further test the performance of the bracket Thermal-Structural ROM over a range of values. First, the ROM was fixed at Yaw = 0° and Applied Force = 66 lbf. ROM deformations and training data were plotted against Pitch over a range of 0 to 90° (Figure 4a). As before, this plot shows good agreement between training data and the developed ROM. Next, the ROM was fixed at Pitch = 15° and Yaw = 30°. ROM deformations and test data were plotted against Applied Force over a range of 0 to 100 lbf (Figure 4a). As before, this plot shows good agreement with some noise present between test data and the developed ROM.



a) ROM results (lines) and training data (markers) versus pitch at Yaw = 0° and Applied Force = 66 lbf.

b) ROM results (lines) and test data (markers) versus applied force at Pitch = 15° and Yaw = 30°.

**Figure 4. Bracket Thermal-Structural performance sweeps.** Performance sweeps of the thermal-structural bracket model for both training and test data.

The success of the sample thermal-structural model provided encouragement for applying the developed method to more complex problems. These are summarized in the following sections.

### III. Case Study: Roman Space Telescope

The Roman Space Telescope (RST) shown in Figure 5 is a NASA observatory designed to settle essential questions in the areas of dark energy, exoplanets, and infrared astrophysics [9]. The optical performance of the RST can be directly tied to thermo-elastic deformations [10] which are expansion/contractions as a result of temperature changes. Consequently, Structural, Thermal, and Optical (STOP) analyses are critical and understanding how thermally induced deformations impact optical performance is paramount. For the current work, we examine thermal-structural interactions; future work is needed to include optical components.

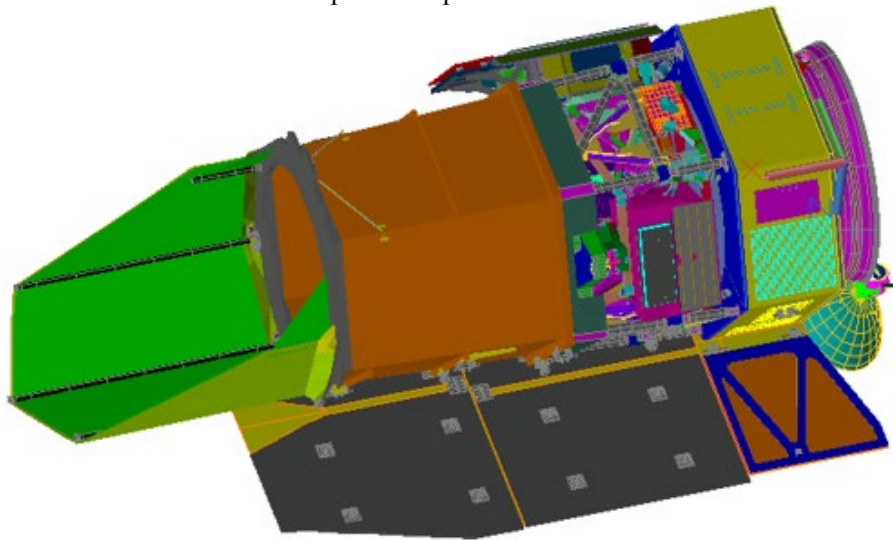


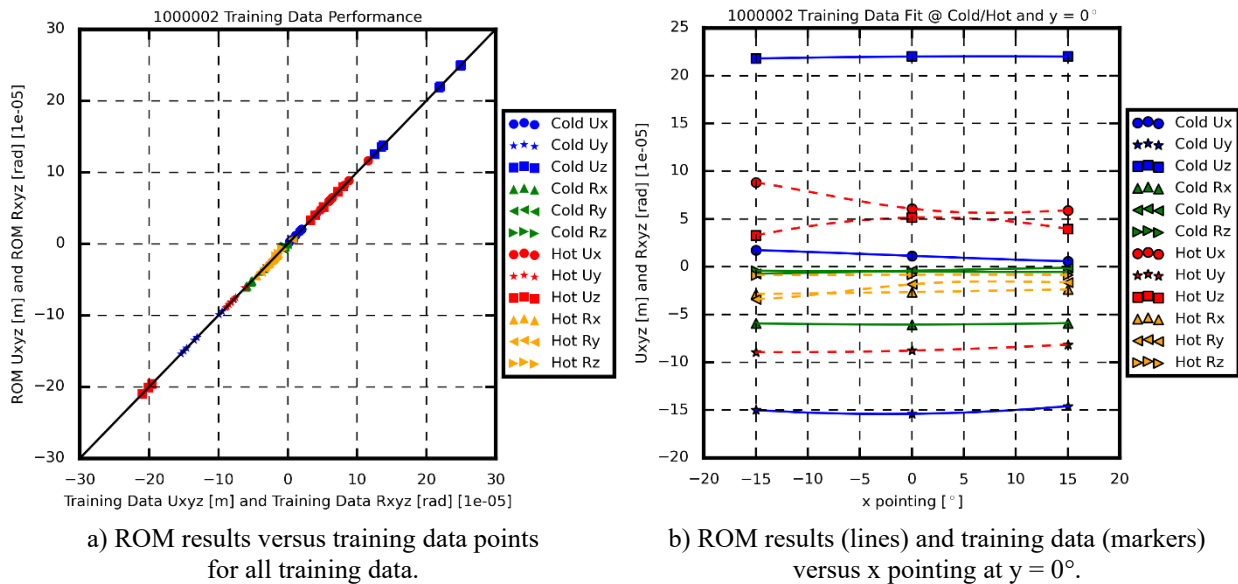
**Figure 5. RST Thermal Desktop® Model.** A ROM was developed based on a 47,278 node Thermal Desktop® and associated NASTRAN model.

As a first step, a multi-disciplinary ROM was developed to better examine how thermal changes impact structural deformations. The RST thermal-structural ROM was developed from a 47,278 node Thermal Desktop model (Figure 5) and associated NASTRAN model. There were 3 input factors (1 categorical and 2 continuous). Input factors include: Hot/Cold cases, y pointing (-36 to 36°), and x pointing (-15 to 15°). There were 42 output responses (6 outputs at each of 7 nodes). These include both displacements (i.e., U) and rotations (i.e., R) as shown below:

- Node 1000002 U<sub>x,y,z</sub> (meters) and R<sub>x,y,z</sub> (radians)
- Node 1001001 U<sub>x,y,z</sub> (meters) and R<sub>x,y,z</sub> (radians)
- Node 1002001 U<sub>x,y,z</sub> (meters) and R<sub>x,y,z</sub> (radians)
- Node 1003001 U<sub>x,y,z</sub> (meters) and R<sub>x,y,z</sub> (radians)
- Node 3740000 U<sub>x,y,z</sub> (meters) and R<sub>x,y,z</sub> (radians)
- Node 3740001 U<sub>x,y,z</sub> (meters) and R<sub>x,y,z</sub> (radians)
- Node 3740002 U<sub>x,y,z</sub> (meters) and R<sub>x,y,z</sub> (radians)

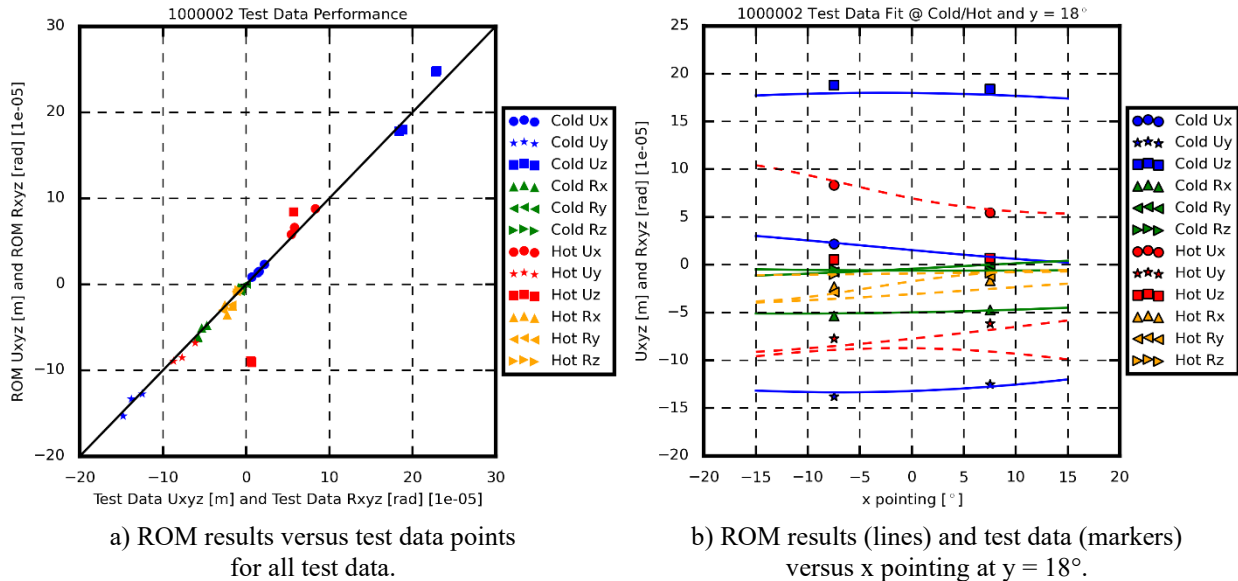
Due to proprietary components, models used in the creation of the RST Thermal-Structural ROM were subsets of the full RST thermal and structural models. The ROM was built using the previously developed intelligent sampling and robust data-fitting methods. Additional Python scripts were developed to aid in processing data. A separate ROM was built for each unique combination of Cold/Hot case, NASTRAN node location, and output response for a total of 84 ROMs. Each of these ROMs was built from 9 training data locations and tested against 3 test points.

Figure 6 shows the performance of the NASTRAN 1000002 ROM (both Cold and Hot cases) against training data points. The figure on the left shows a direct comparison for all training data points (deformations and rotations). Data points falling on a 45° line indicate perfect agreement. The figure on the right shows a comparison of the ROM results (i.e., lines) and training data points (i.e., markers) over a sweep of the x pointing input factor at y = 0°. The ROM results match very well with the training data, which is expected since the ROMs were built with a zero-noise variance.



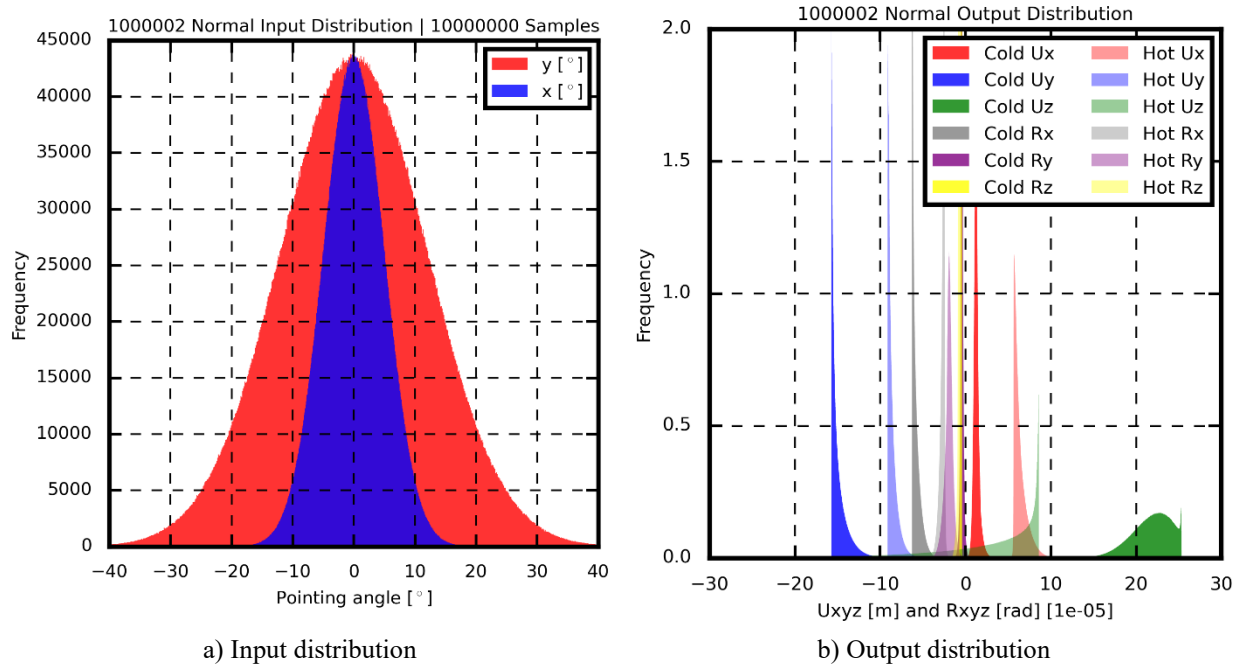
**Figure 6. Training Data performance.** Performance of the NASTRAN 1000002 ROM (both Cold and Hot cases) against training data points.

Next, ROM results were compared to the test runs (Figure 7). Test cases were not used to develop the ROM and therefore provide a good check of ROM performance. These figures show good agreement for most output responses, although the Hot Uz (z displacement) test output deviates the most (i.e., 9.8e-5 m). The Hot Uz test result could likely be remedied with slightly more training data which would improve the fit in that region.



**Figure 7. Test Data performance.** Performance of the NASTRAN 1000002 ROM (both Cold and Hot cases) against test data points.

Advanced analysis capabilities (e.g., Uncertainty Quantification) were then demonstrated. Input factors were given a distribution with an assumed uncertainty. For example, it was assumed that expected y and x rotations would be  $0^\circ$ ; however, it was an uncertain value that could be higher and lower. Because of this, a normal input distribution centered at  $0^\circ$  for the y and x pointing angles was applied with standard deviations of  $12^\circ$  and  $5^\circ$ , respectively. These were arbitrarily selected to ensure the distribution captured the range of the input factors (i.e.,  $-36$  to  $36^\circ$  and  $-15$  to  $15^\circ$ ). Using this approach, pointing angles at  $0^\circ$  are most likely to occur and those at the extents (e.g., y pointing =  $-36^\circ$ ) are least likely. The resulting distributions for node 1000002 are shown in Figure 8. This input factor distribution (Figure 8a) was then applied to the RST Thermal-Structural ROM (Cold- and Hot-cases) and the output distributions (Figure 8b) were plotted (within a few seconds).



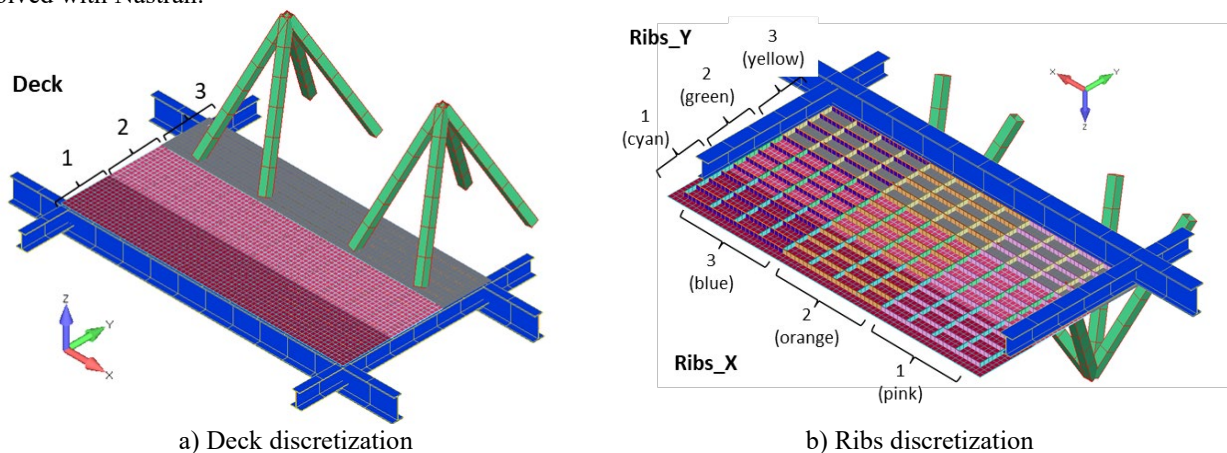
**Figure 8. Uncertainty Quantification.** Evaluation of input factor uncertainty can be applied to a Thermal-Structural system.



Figure 8 shows how an uncertain input (e.g., pointing) can be used to better understand its impact to an output response (e.g., displacement/rotations). Using the RST Thermal-Structural ROM, these results can be obtained in a few seconds for 10,000,000 samples. It should be noted that other input distributions (e.g., uniform) and/or shapes (e.g., 3° standard deviation) could quickly be implemented with this method. These results illustrate the power of reduced-order modeling. Within just a few seconds, we not only determine the extents of deformations/rotations but can also see their unique distributions. These distributions can let users assign probabilities to outputs.

#### IV. Case Study: Structural Platform

To further test the developed methods, a purely structural case was identified. The model (Figure 9) represents two chairs fixed upon a beam-supported structural platform. The platform consists of a deck with ribs on the underside (i.e., -z). Plate elements were used to construct the deck and ribs, while beam elements were used for the supports and chair legs. A ~200 lb. point mass is connected at the top of each chair. All components were assumed to have Al7050 material properties and strength characteristics. The finite element model was built using Simcenter FEMAP and solved with Nastran.



**Figure 9. Structural Model.** A finite element model was built using Simcenter FEMAP and solved with Nastran.

The model is constrained in the translation DOFs at each support beam end and at each chair leg. The two chair legs that sit on the platform are directly attached to the platform elements, analogous to being bolted down to the floor. Three separate acceleration load cases were considered for this analysis which include: 1) Forward crash (10G in -x direction), 2) Side crash (5G in +y direction), and Down crash (20G in -z direction). In each case a 1.5 psi pressure load is applied to the platform surface. This represents cargo weighing roughly 2,000 lbs. sitting on the platform. To develop the Structural ROM, 9 input and 2 output parameters were identified to track and vary in the study. These include:

- 3 Deck Thicknesses (0.03 to 0.3 in)
- 3 Rib Thicknesses (x-direction) (0.03 to 0.3 in)
- 3 Rib Thicknesses (y-direction) (0.03 to 0.3 in)

These inputs are illustrated in Figure 9. The model has a corresponding property card which defines the material and thickness of each element group. This information can be edited outside of FEMAP, allowing for easy modification of input files (.dat) to generate many simulations with different thickness combinations. The key outputs of interest in the analysis were the mass of the platform and maximum Von Mises (VM) stresses in the structure. During the analysis solution process, the mass of the full model is written to an output file (.f06) as well as the VM stress for every element in each of the three load cases.

1,152 different simulations were analyzed to generate training data (1,024 points), validation data (100 points), and test data (28 points). Each simulation runs through the three acceleration load cases, taking about 10 seconds each. The time required to solve all the different simulations was about 3 hours. The resulting solution set contains mass and stresses as a function of the 9 input factors. A Python script was developed to parse through the input and output

files for each simulation and build a CSV table with a row for each containing the 9 input factors, mass, and maximum overall VM stress. A Structural ROM was developed using existing robust data fitting methods.

Evaluation of this complex system was first done by generating an optimization plot (Figure 10a) in Veritrek against the two output responses (Maximum Stress and Panel Mass) for the full range of thickness (i.e., 0.03 to 0.3 inches). The goal of this structural platform analysis is to minimize panel mass while staying within maximum stress limits. This plot shows an optimal Pareto front of maximum stress and panel mass and could be used to help optimize the design.

Next, a screening analysis was conducted in Veritrek to show the relative importance of each input factor on the Maximum Stress output response. This plot demonstrates that the thickness of the Deck in area 3 (refer to Figure 10b) is the most impactful on Maximum Stress. Secondly is the Deck thickness in area 2. By using the screening analysis, a design engineer could use these results to help focus their efforts on critical areas and could lead to improved designs (e.g., adding structural stiffeners in Deck area 2 and 3).

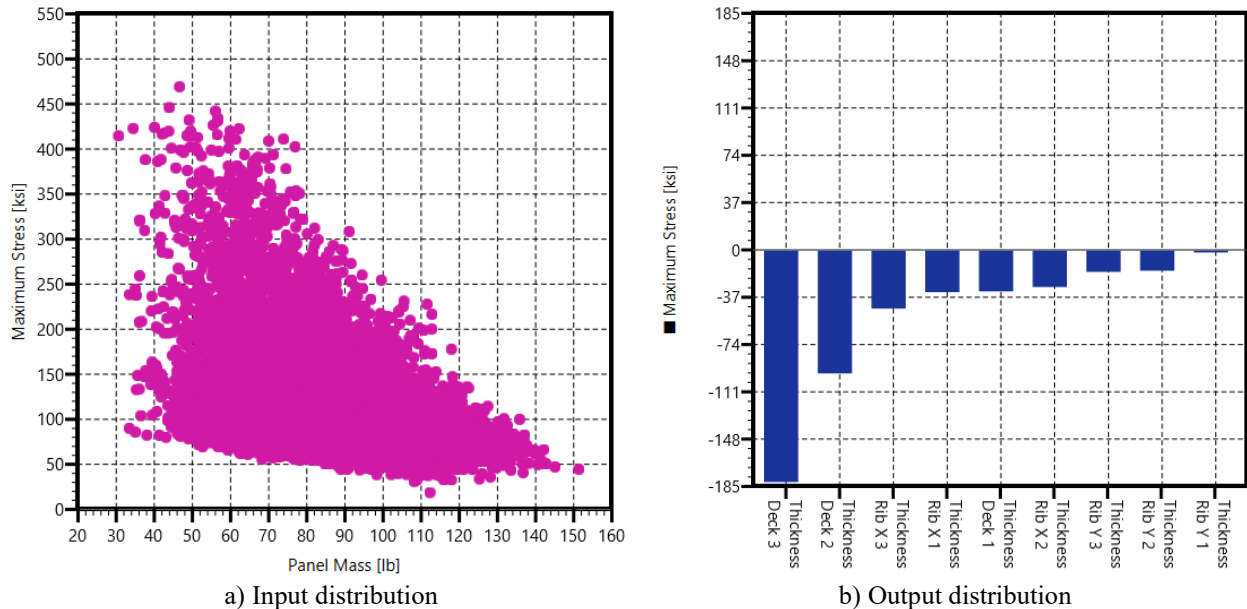


**Figure 10. Optimization and Screen Studies.** *Evaluation of advanced analyses can be applied to a structural system.*

## V. Conclusions and Future Development

Previous reduced-order modeling approaches were expanded to include structural analyses. The result included methods to create both Thermal-Structural and Structural-only ROMs. These methods were tested against a sample bracket thermal-structural problem and showed good agreement between ROM and training/test results. These same methods were expanded to a more complex design in the Roman Space Telescope (RST). An RST Thermal-Structural ROM was built and showed good performance. By leveraging the utility of a ROM, analyses such as Uncertainty Quantification (UQ) are readily available. Using ROMs and UQ methods, the distribution of expected RST displacement/rotations were illustrated over a broad range of pointing conditions. This work concluded by demonstrating these same methods for a structural-only problem. The developed Structural-ROM was able to help identify Pareto front optimal conditions and quickly ascertain critical thickness that impact maximum stress values. Expanding ROM capabilities to include thermal and structural analyses has the potential to benefit a broad range of engineering applications. The capabilities would give engineers the ability to better evaluate uncertainties, help identify more optimal solutions, and quickly identify critical design inputs.

## Acknowledgments

This material is based upon work supported by Small Business Innovative Research projects with NASA. A special thanks is given to Michael Akkerman for the generation of a simplified structural NASTRAN FEM for RST to allow this effort to proceed.



## References

1. Hengeveld, D. and J. Moulton. *Uncertainty Quantification Using Reduced-Order Models*. in *49th International Conference on Environmental Systems*. 2019. 49th International Conference on Environmental Systems.
2. Hengeveld, D. and J. Moulton. *Automatic creation of reduced-order models using Thermal Desktop®*. in *48th International Conference on Environmental Systems*. 2018. 48th International Conference on Environmental Systems.
3. Hengeveld, D.W. and A. Biskner. *Enhanced data exploration through Reduced-Order Models*. in *47th International Conference on Environmental Systems*. 2017. Charleston, South Carolina.
4. Hengeveld, D.W. *Reduced-Order Modeling for Rapid Thermal Analysis and Evaluation of Spacecraft*. in *46th AIAA Thermophysics Conference*. 2016.
5. Hengeveld, D.W. *Reduced-Order Modeling for Rapid Thermal Analysis and Evaluation of Spacecraft*. in *2016 Thermal & Fluids Analysis Workshop (TFAWS)*. 2016. Moffet Field, CA.
6. Cappucci, S., J.A. Moulton, and D.W. Hengeveld. *Assessment of the Mars Helicopter Thermal Design Sensitivities using the Veritrek Software*. in *2018 Thermal & Fluids Analysis Workshop (TFAWS)*. 2018. Galveston, TX.
7. Cappucci, S., J.A. Moulton, and D.W. Hengeveld. *Assessment of the Mars Helicopter Thermal Design Sensitivities using the Veritrek Software*. in *2018 Thermal & Fluids Analysis Workshop (TFAWS)*. 2018. Galveston, TX.
8. Hengeveld, D.W. and J.A. Moulton. *Automatic creation of reduced-order models using Thermal Desktop®*. in *2018 Thermal & Fluids Analysis Workshop (TFAWS)*. 2018. Galveston, TX.
9. NASA. [cited 2021 February 24]; Available from: <https://roman.gsfc.nasa.gov/about.html>.
10. Poberezhskiy, I., et al. *Roman space telescope coronagraph: engineering design and operating concept*. in *Space Telescopes and Instrumentation 2020: Optical, Infrared, and Millimeter Wave*. 2021. SPIE.